MedCrave
Step into the World of Research

MOJ Applied Bionics and Biomechanics

Research Article

Open Access

CrossMark

Modeling and simulation to predict variation of void ration and permeability influence on *E-coli* transport in heterogeneous sand gravel depositions

Abstract

This study monitored heterogeneous deposition of void ratio in predominant sand gravel depositions, several studies had been done on transport system with relation to depth of the formation, but the study centered more on time of transport in relation to heterogeneous void ratio and permeability of sand gravel formation, the time of transport were subjected to determine the rate of transport to the Phreatic depositions, fluctuation and exponential phase of transport were observed in the study area, depth of transport were slightly evaluated in the study, but the focus of the study is more on time influenced by heterogeneous void ratio on sand gravel depositions, simulation generated predictive values that were validated with experimental values and both parameters express favorable fits for model validation, the study provide platform to monitor time of transport influenced by heterogeneous void ratio in predominant sand grave depositions. Experts will definitely use the concept to monitor time of transport of *E-Coli* in sand gravel formation.

Keywords: modeling variation void ratio, permeability, *E-Coli*, transport and sand gravel formation

Volume 2 Issue 5 - 2018

Eluozo SN,[1] Afiibor BB[2]

[1]Department of Civil Engineering, Gregory University Uturu (GUU), Nigeria
[2]Department of Statistics Federal Polytechnic, Nigeria

Correspondence: Eluozo SN, Department of Civil Engineering, Gregory University Uturu (GUU), Abia State of Nigeria, Nigeria, Email Soloeluozo2013@hotmail.com

Received: August 31, 2018 | **Published:** October 08, 2018

Introduction

The behaviour of soil base on evaluation tools known as (SWAT)[1,2] was effectively applied to simulate river flow micronutrient were found from evaluation of the Rivers,[3] and *E. coli* fluxes.[4-6] The integration of this model was done in landscape which also includes in-stream microbial processes, this concept was thoroughly applied in other to simulate management scenarios in degradation of contamination.[2,3,7] The programme called SWAT permit modeling of bacteria fate and transport. even though calibration of the model for faecal fluxes seems more difficult compare to flow, it may be due to the paucity of data and inadequate understanding of *E. coli* biophysical process, this concept has definitely signify most important breakthrough on approximation *E. coli* fluxes.[4,8] The system of developing modeling in regional degree has been an adopted concept in the past years by Lazure and Dumas,[9] this concept was to explain currents, dilution and transport im most parts of the French coast. In recent times, it was observed that water quality variations have been realizeed, this was observed in some particular faecal contamination through bathing and shellfish harvesting areas.[7-9] These concept currently applied models is to manage the impact of wastewater on the sea water.[10] Expressing such knowledge has been applied to monitor the system daily flows that are simulated with a watershed model as an input into another hydrodynamic model to assess daily bacterial concentrations in estuaries.[11,12] These the two conceptual model applications are used to monitor microbiological contamination in an estuary, which is crucial for coastal management.

Theoretical background

$$V\Phi\frac{\partial c}{\partial t} = KV_t\frac{\partial^2 c}{\partial x^2} - K_d\frac{\partial c}{\partial x} \quad (1)$$

Nomenclature

C=*E.Coli* Concentration

K =Permeability

V =Velocity

Φ =Porosity

K_d =Decay Rate

x =Depth

T =Time

Let C =TX

Applying Bernoulli's method of separation of variables

$$V\Phi\frac{T^1}{T} = KV_t X^{11} - K_d X^1 = \beta^2 \quad (2)$$

$$V\Phi\frac{T^1}{T} = \beta^2 \quad (3)$$

$$KV_t X^{11} - K_d X^1 - \beta^2 X = 0 \quad (4)$$

From $T = a\ell^{\frac{\beta^2}{KV_t}t}$ (5)

From (4), the auxiliary equation is

$$KV_t M^2 - K_d M - \beta^2 = 0$$

$$M = \frac{K_d \pm \sqrt{K_d^2 + 4KV_t\beta^2}}{2V\Phi} \quad (6)$$

Hence, we have

$$X = ACos\,Mx + BSin\,Mx \quad (7)$$

Combining (3) and (4), we have: -

$$C(x,t) = a\ell V\Phi^{\frac{\beta^2}{t}}\left[ACos\,Mx + BSin\,Mx\right] \quad (8)$$

Subject equation (8) to boundary condition

$at \quad x=0 \quad c=0$ Yield: -

$0 = aA$

i.e. $C(x,t) = a\ell V\Phi^{\frac{\beta^2}{t}}\left[ACos\,Mx + BSin\,Mx\right] \quad (9)$

$$\frac{\partial c}{\partial x} = C_o\ell V\Phi^{\frac{\beta^2}{t}}\left[-AMSin\,Mx + BMCos\,Mx\right]$$

At $x=0, \frac{\partial c}{\partial x} = 0$

$$o = C_o\ell V\Phi^{\frac{\beta^2}{t}}(Cos\,Mx) \quad (10)$$

At $x=L, \frac{\partial c}{\partial L} = 0$ yields: -

$$o = C_o\ell V\Phi^{\frac{\beta^2}{t}}\left[-AMSin\,ML\right] \quad (11)$$

$$C_o\ell V\Phi^{\frac{\beta^2}{t}} \neq 0$$

$$AMSin\,L = 0 = n\pi, n = 1,2,3$$

$$ML = n\pi \quad m = \frac{n\pi}{L}$$

$$C(x,t) = Co\ell V\Phi^{\frac{\beta^2}{t}}\left[Cos\frac{M\pi}{L}x\right] \quad (12)$$

If $x = V \cdot t$

$$C(x,t) = Co\ell V\Phi^{\frac{\beta^2}{t}}\left[Cos\frac{M\pi}{L}V \cdot t\right] \quad (13)$$

If $t = \frac{d}{v}$

$$C(x,t) = Co\ell V\Phi^{\frac{\beta^2}{t}}\left[Cos\frac{M\pi}{L}\frac{d}{v}\right]$$

Materials and method

Standard laboratory experiment where performed to monitor the concentration of *E-Coli* transport at different formation. The soil deposition of the strata was collected in sequences based on the structural deposition at different locations. The samples collected at different locations generated variations at different depth producing different migration of *E-Coli* concentration through pressure flow at the lower end of the column. The experimental result are applied and compared with the theoretical values for model validation.

Results and discussion

Results are presented in tables and figures including graphical representation of *E-Coli* concentration. Figure 1 express gradual increase of the predictive *E-Coli* concentration from ten to forty days and suddenly experienced decrease with increase in time to lowest rate concentration recorded at one hundred and twenty days, while the experimental values gradual decrease from the optimum values recorded at ten to the lowest concentration observed at the same period, Figure 2 predictive values experienced fluctuation where the optimum values was observed at ninety day and final decrease down to the lowest rate of concentration recorded at one twenty days, while the experimental values maintained fluctuation but at different time to the lowest concentration recorded at the same time. Figure 3 observed similar condition but at different time, fluctuation were experienced from ten to two hundred days, where the lowest concentration were observed, while that of experimental values maintained similar condition, but experience higher concentration compared to that of the predictive. Figure 4 developed an exponential phase of the system were the optimum values were recorded sixty metres, while the experimental values maintained the same trend to the optimum parameters recorded at the same depth. Figure 5 predictive maintained linear increase with increase in depth to the optimum values observed at sixty metres, while that of the experimental values experienced vacillation from nine to forty days and linearly increase to the optimum at thirty nine days, Figure 6 observed gradual increase and suddenly experience decrease to lowest rate of concentration. While that of the experimental values increase in similar condition to the optimum values at hundred and fifty days, but suddenly experienced slight decrease between hundred and sixty to two hundred days, while Figure 7 gradually increase with depth to the optimum values recorded at thirty six metres and suddenly experiences decrease to the lowest concentration recorded at sixty metres, while that of the experimental values maintained the same trend of concentration to the lowest depth at sixty metres. Figure 8 predictive and experimental values developed fluctuation from twenty four to sixty metres, Figure 9 predictive observed different concentration in migration, and both parameters observed gradual increase to the optimum values recorded at two hundred days (Tables 1-10).

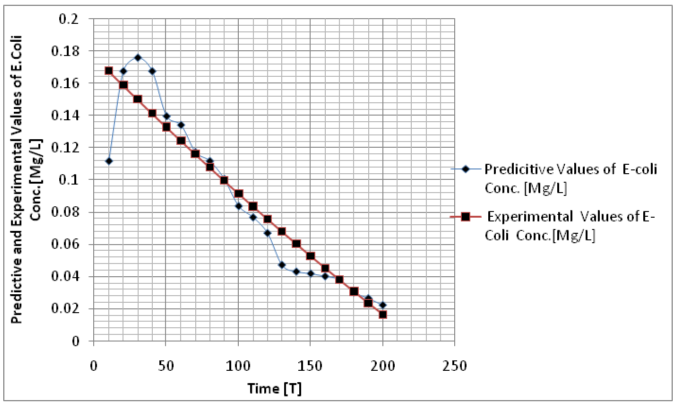

Figure 1 Predictive and experimental values of *E-Coli* concentration at different depth.

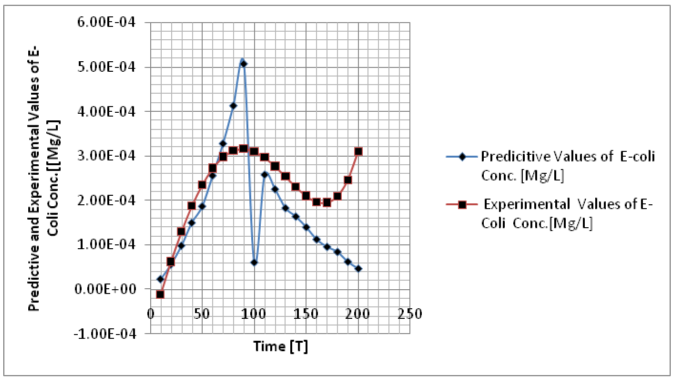

Figure 2 Predictive and experimental values of *E-Coli* concentration at different time.

Citation: Eluozo SN, Afiibor BB. Modeling and simulation to predict variation of void ration and permeability influence on *E-coli* transport in heterogeneous sand gravel depositions. *MOJ App Bio Biomech.* 2018;2(5):295–301. DOI: 10.15406/mojabb.2018.02.00084

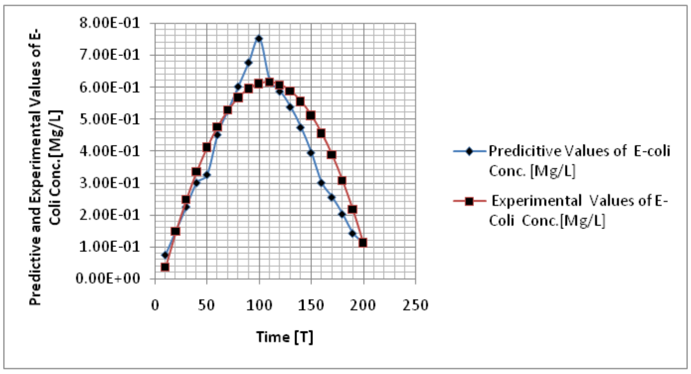

Figure 3 Predictive and experimental values of *E-Coli* concentration at different time.

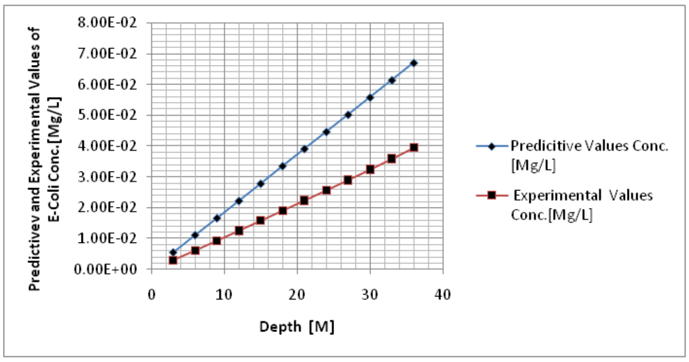

Figure 4 Predictive and experimental values of *E-Coli* concentration at different depth.

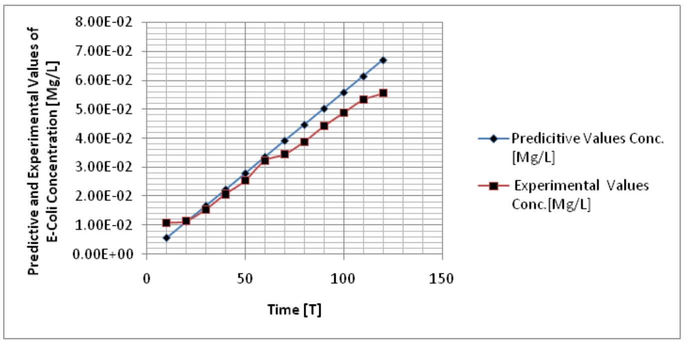

Figure 5 Predictive and experimental values of *E-Coli* concentration at different time.

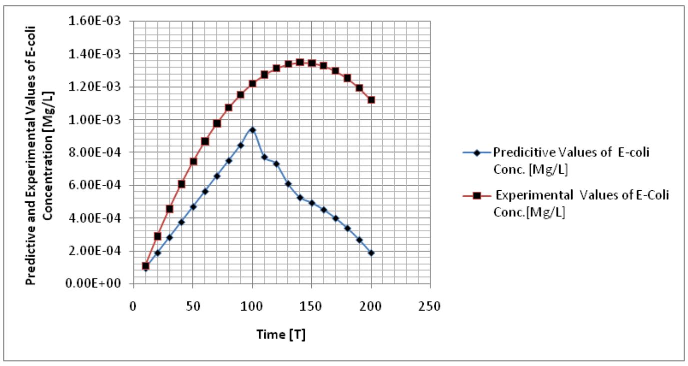

Figure 6 Predictive and experimental values of *E-Coli* concentration at different time.

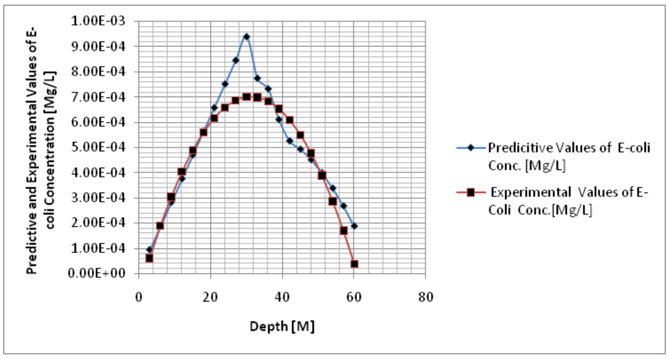

Figure 7 Predictive and experimental values of *E-Coli* concentration at different depth.

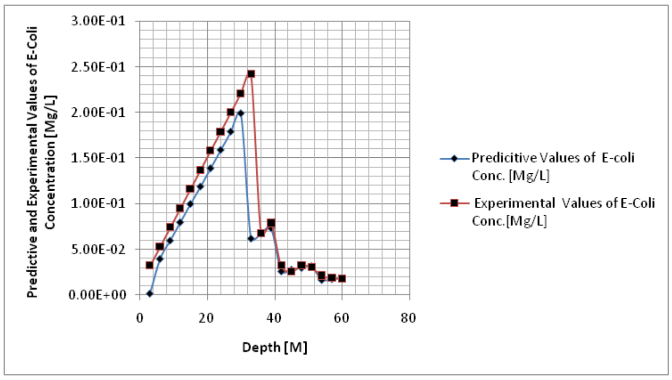

Figure 8 Predictive and experimental values of *E-Coli* Concentration at different depth.

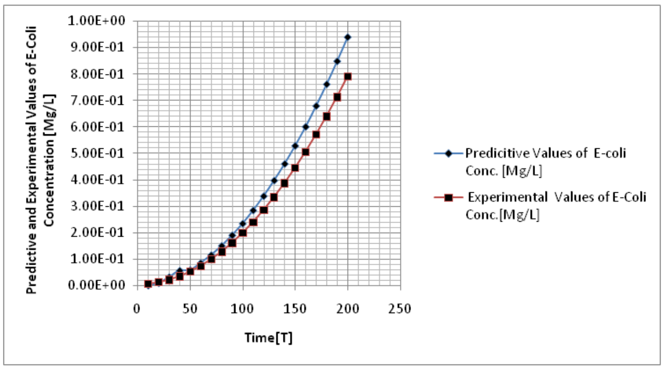

Figure 9 Predictive and experimental values of *E-Coli* concentration at different depth.

Table 1 Predictive and experimental values of *E-coli* concentration at different time

Time [T]	Predictive values of *E-coli* conc. [Mg/L]	Experimental values of *E-Coli* conc.[Mg/L]
10	0.1119	0.16765
20	0.1678	0.1588
30	0.1762	0.15005
40	0.1678	0.1414
50	0.1398	0.13285
60	0.1343	0.1244

Table Continued....

Time [T]	Predictive values of *E-coli* conc. [Mg/L]	Experimental values of *E-Coli* conc.[Mg/L]
70	0.1175	0.11605
80	0.1119	0.1078
90	0.1007	0.09965
100	0.0839	0.0916
110	0.0769	0.08365
120	0.0671	0.0758
130	0.0473	0.06805
140	0.0431	0.0604
150	0.0419	0.05285
160	0.0402	0.0454
170	0.0381	0.03805
180	0.0302	0.0308
190	0.0265	0.02365
200	0.0223	0.0166

Table 2 Predictive and experimental values of *E-coli* concentration at different time

Time [T]	Predictive values of *E-coli* conc. [Mg/L]	Experimental values of *E-Coli* conc.[Mg/L]
10	2.34E-05	-0.00001148
20	5.63E-05	0.00006232
30	9.86E-05	0.00012912
40	1.50E-04	0.00018712
50	1.87E-04	0.000235
60	2.56E-04	0.00027192
70	3.28E-04	0.00029752
80	4.13E-04	0.00031192
90	5.07E-04	0.00031572
100	6.10E-05	0.00031
110	2.58E-04	0.00029632
120	2.25E-04	0.00027672
130	1.83E-04	0.00025372
140	1.64E-04	0.00023032
150	1.40E-04	0.00021
160	1.13E-04	0.00019672
170	9.58E-05	0.00019492
180	8.45E-05	0.00020952
190	6.25E-05	0.00024592
200	4.70E-05	0.00031

Table 3 Predictive and experimental values of *E-coli* concentration at different time

Time [T]	Predictive values of *E-coli* conc. [Mg/L]	Experimental values of *E-Coli* conc.[Mg/L]
10	7.54E-02	0.036
20	1.51E-01	0.148
30	2.26E-01	0.248
40	3.02E-01	0.336
50	3.27E-01	0.412
60	4.52E-01	0.476
70	5.28E-01	0.528
80	6.03E-01	0.568
90	6.79E-01	0.596
100	7.54E-01	0.612
110	6.22E-01	0.616
120	5.88E-01	0.608
130	5.39E-01	0.588
140	4.75E-01	0.556
150	3.96E-01	0.512
160	3.02E-01	0.456
170	2.56E-01	0.388
180	2.04E-01	0.308
190	1.43E-01	0.216
200	1.13E-01	0.112

Table 4 Predictive and experimental values of *E-coli* concentration at different depth

Depth [M]	Predictive values conc. [Mg/L]	Experimental values conc.[Mg/L]
3	5.59E-03	3.05E-03
6	1.12E-02	6.18E-03
9	1.67E-02	9.36E-03
12	2.23E-02	1.26E-02
15	2.79E-02	1.58E-02
18	3.36E-02	1.91E-02
21	3.92E-02	2.24E-02
24	4.47E-02	2.57E-02
27	5.03E-02	2.90E-02
30	5.59E-02	3.24E-02
33	6.15E-02	3.59E-02
36	6.71E-02	3.95E-02

Table 5 Predictive and experimental values of *E-coli* concentration at different depth

Time [T]	Predictive values conc. [Mg/L]	Experimental values conc.[Mg/L]
10	5.59E-03	1.10E-02
20	1.12E-02	1.15E-02
30	1.67E-02	1.55E-02
40	2.23E-02	2.08E-02
50	2.79E-02	2.54E-02
60	3.36E-02	3.23E-02
70	3.92E-02	3.45E-02
80	4.47E-02	3.88E-02
90	5.03E-02	4.42E-02
100	5.59E-02	4.88E-02
110	6.15E-02	5.33E-02
120	6.71E-02	5.55E-02

Table 6 Predictive and experimental values of *e-coli* concentration at different depth

Time [T]	Predictive values of *E-coli* conc. [Mg/L]	Experimental values of *E-Coli* conc.[Mg/L]
10	9.39E-05	0.000113
20	1.88E-04	0.000292
30	2.82E-04	0.000457
40	3.76E-04	0.000608
50	4.70E-04	0.000745
60	5.63E-04	0.000868
70	6.57E-04	0.000977
80	7.51E-04	0.001072
90	8.45E-04	0.001153
100	9.39E-04	0.00122
110	7.74E-04	0.001273
120	7.32E-04	0.001312
130	6.10E-04	0.001337
140	5.26E-04	0.001348
150	4.93E-04	0.001345
160	4.51E-04	0.001328
170	3.99E-04	0.001297
180	3.38E-04	0.001252
190	2.68E-04	0.001193
200	1.88E-04	0.00112

Table 7 Predictive and Experimental Values of *E-Coli* Concentration at Different Depth

Depth [M]	Predictive values of *E-coli* conc. [Mg/L]	Experimental values of *E-Coli* conc.[Mg/L]
3	9.39E-05	6.28E-05
6	1.88E-04	1.91E-04
9	2.82E-04	3.05E-04
12	3.76E-04	4.05E-04
15	4.70E-04	4.90E-04
18	5.63E-04	5.61E-04
21	6.57E-04	6.17E-04
24	7.51E-04	6.59E-04
27	8.45E-04	6.87E-04
30	9.39E-04	7.00E-04
33	7.74E-04	6.99E-04
36	7.32E-04	6.83E-04
39	6.10E-04	6.53E-04
42	5.26E-04	6.09E-04
45	4.93E-04	5.50E-04
48	4.51E-04	4.77E-04
51	3.99E-04	3.89E-04
54	3.38E-04	2.87E-04
57	2.68E-04	1.71E-04
60	1.88E-04	4.00E-05

Table 8 Predictive and experimental values of *E-Coli* concentration at different depth

Depth [M]	Predictive values of *E-coli* conc. [Mg/L]	Experimental values of *E-Coli* conc.[Mg/L]
3	1.99E-03	3.20E-02
6	3.99E-02	5.30E-02
9	5.99E-02	7.40E-02
12	7.99E-02	9.50E-02
15	9.99E-02	1.16E-01
18	1.19E-01	1.37E-01
21	1.39E-01	1.58E-01
24	1.59E-01	1.79E-01
27	1.79E-01	2.00E-01
30	1.99E-01	2.21E-01
33	6.21E-02	2.42E-01
36	6.77E-02	6.77E-02
39	7.34E-02	7.88E-02
42	2.63E-02	3.22E-02
45	2.81E-02	2.55E-02
48	3.01E-02	3.22E-02
51	3.19E-02	3.05E-02
54	1.69E-02	2.11E-02
57	1.79E-02	1.89E-02
60	1.88E-02	1.78E-02

Table 9 Predictive and experimental values of E-Coli concentration at different time

Time [T]	Predictive values of *E-coli* conc. [Mg/L]	Experimental values of *E-Coli* conc.[Mg/L]
10	2.34E-04	0.0063
20	9.23E-03	0.0116
30	3.17E-02	0.0209
40	5.63E-02	0.0342
50	5.87E-02	0.0515
60	8.46E-02	0.0728
70	1.15E-01	0.0981
80	1.50E-01	0.1274
90	1.90E-01	0.1607
100	2.34E-01	0.198
110	2.84E-01	0.2393
120	3.38E-01	0.2846
130	3.97E-01	0.3339
140	4.60E-01	0.3872
150	5.28E-01	0.4445
160	6.00E-01	0.5058
170	6.79E-01	0.5711
180	7.61E-01	0.6404
190	8.48E-01	0.7137
200	9.39E-01	0.791

Table10 Predictive and experimental Values of E-Coli concentration at different depth

Depth [M]	Predictive values of *E-Coli* conc. [Mg/L]	Experimental values of *E-Coli* conc.[Mg/L]
3	4.85E-05	0.000115858
6	1.93E-04	0.000260602
9	4.35E-04	0.000354406
12	7.74E-04	0.000406666
15	1.21E-04	0.000426
18	1.74E-04	0.00042025
21	2.37E-04	0.000396478
24	3.09E-04	0.00036097
27	3.92E-04	0.000319234
30	4.84E-04	0.000276
33	5.59E-05	0.000235222
36	6.65E-05	0.000200074
39	7.81E-05	0.000172954
42	9.05E-05	0.000155482
45	1.06E-06	0.0001485
48	1.18E-06	0.000152074
51	1.34E-06	0.00016549
54	1.49E-06	0.000187258
57	1.66E-06	0.00021511
60	1.84E-06	0.000246

Conclusion

The study has express the behavior of the system in terms of deposition under variation of permeability and void ratio in *E-coli* transport , the litho structure in the study environment express heterogeneous deposition under the influences of heterogeneous void ratio in sand grave formation, such condition were observed to pressure the transport behaviors of *E-coli* in sand grave depositions, exponential and fluctuation were experienced reflecting the litho structure of the predominant sand gravel deposition, the contaminant were found to pressure in transport process to Phreatic depositions, the study observed variation of micronutrient in different deposition, these are experienced in aquitard and unconfined deposition in Phreatic regions, the study centered more on time of transport under these lithology in the study environment, these condition implies that time and structural setting determined rapid rate of transport to Phreatic beds, these expression detailed the behavior of the transport system in sand gravel region of the study area. Other studies have base more on the depth of the formation, but time in relation to structural depositions has not monitored in detail, this study express the simulation of transport time more than that depth of the transport process, the simulation defined the system process of void ratios in heterogeneous condition, it also express the void ratio heterogeneous setting in sand gravel depositions, simulation developed some high percentage of favorable fits. The study has predicted time relationship with heterogeneous setting of void ratios in sand gravel formation.

Acknowledgements

None.

Conflict of interest

Authors declare there is no conflict of interest in publishing the article.

References

1. Arnold JG, Fohrer N. SWAT2000: current capabilities and research opportunities in applied watershed modelling. *Hydrological Processes*. 2005;19:563–572.
2. Arnold JG, Srinivasan R, Muttiah RS, et al. Large area hydrologic modeling and assessment part i: model development. *Journal of the American water resources association*. 1998;34(10):73–89.
3. Pohlert T, Huisman JA, Breuer L, et al. Modelling of point and non–point source pollution of nitrate with SWAT in the river Dill, Germany. *Advances in Geosciences*. 2005;5:7–12.
4. Baffaut C, Benson VW. A Bacteria TMDL for Shoal Creek Using Swat Modeling and DNA Source Tracking. In: *Total Maximum Daily Load (TMDL) Environmental Regulations II*. ASAE Conference Proceedings, Albuquerque, New Mexico, editor A Saleh; 2003. p. 35–40
5. Guber AK, Pachepsky YA, Sadeghi AM. Evaluating uncertainty in *E. coli* retention in vegetated filter strips in locations selected with SWAT simulations. *in* ASABE, editor. *Watershed Management to Meet Water Quality and TMDLS*. San Antonio, Texas; 2007.p. 286–293.
6. Parajuli P, Mankin KR, Barnes PL. New methods in modeling source–specific bacteria at watershed scale using SWAT. In: Watershed Management to meet Water Quality Standards and TMDLs (Total Maximum Daily Load) Proceedings. ASABE 830 Publication No. 701P0207. St. Joseph, MI: ASABE; 2007.
7. Morgane Bougeard, Jean–Claude Le Saux, Nicolas Pérenne Monique Pommepuy. Modeling of *Escherichia coli* Fluxes on a catchment and the impact on coastal water and shellfish quality. *Journal American water resources association*. 2011;47(2):P350–366.

8. Parajuli P. *SWAT bacteria sub–model evaluation and application – an abstract of a dissertation*. Department of Biological and Agricultural Engineering, College of Engineering, Manhattan, Kansas: Kansas State University; 2007. p. x–212.
9. Riou P, Le Saux JC, Dumas F, et al. Microbial impact of small tributaries on water and shellfish quality in shallow coastal areas. *Water Research*. 2007;41(12):2774–2786.
10. Fiandrino AY, Martin P, Got JL, et al. Bacterial contamination of Mediterranean coastal seawater as affected by riverine inputs: simulation approach applied to a shellfish breeding area (Thau lagoon, France). *Water Research*. 2003;37(8):1711–1722.
11. Hooda PS, Edwards AC, Anderson HA, et al. A review of water quality concerns in livestock farming areas. *The Science of the Total Environment*. 2000;250(1–3):143–167.
12. Parajuli P, Mankin KR, Barnes PL. Source specific fecal bacteria modeling using soil and water assessment tool model. *Bioresource Technology*. 2009;100(2):953–963.